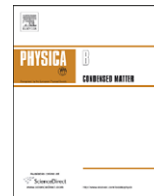




Contents lists available at ScienceDirect

Physica B

journal homepage: www.elsevier.com/locate/physb

Detailed hyperfine structure of muoniated radicals in planar phthalocyanines

J. Piroto Duarte^{a,b,*}, R.C. Vilão^b, H.V. Alberto^b, J.M. Gil^b, A. Weidinger^b, N. Ayres de Campos^b^a E.S.Te.S.C., Polytechnic Institute of Coimbra, P-3040-854 Coimbra, Portugal^b CEMDRX, Department of Physics, University of Coimbra, P-3004-516 Coimbra, Portugal

ARTICLE INFO

Keywords:

Organic semiconductors
Phthalocyanine
Muon spin rotation
Muoniated radicals

ABSTRACT

A detailed report of the hyperfine structure of paramagnetic muoniated radicals in the planar phthalocyanine zinc phthalocyanine (ZnPc) is given in this work. The hyperfine parameters of the three muoniated radical states formed in this compound were determined from high transverse-field μ SR measurements of a polycrystalline sample, taking into account the axial symmetry of the hyperfine tensor. States I and II are seen to possess a small dipolar character, consistent with the delocalization of the radical's electron to the inner ring of the phthalocyanine molecule, while state III has a hyperfine structure similar to the Mu_{BC} centre formed in inorganic semiconductors. This suggests that the muon in state III occupies an interstitial position between two stacked phthalocyanine molecules.

© 2008 Elsevier B.V. All rights reserved.

1. Introduction

Planar phthalocyanines consist of a π -conjugated macrocycle ligand (Pc) with a central cavity where a metallic atom may be bonded (Fig. 1) [1]. The μ SR signal of phthalocyanines with non-magnetic inclusions is known from the study of the metal-free phthalocyanine (H_2Pc) and zinc phthalocyanine (ZnPc), where three distinct muoniated radicals, labeled I–III, have been observed [2,3]. Their hyperfine constants were established in Ref. [2] using an isotropic description of the hyperfine interaction, but a detailed characterization of the hyperfine structure was recently found to be necessary in order to understand the spin-dynamics of those states in longitudinal-field geometry [4].

This work presents a description of the hyperfine structure of states I–III in ZnPc considering an axially symmetric description for the hyperfine interaction of the states.

2. Experimental details

The μ SR results discussed here were taken with phthalocyanine samples of ZnPc prepared from polycrystalline material acquired from Alfa Aesar in a nominally pure grade (98%), purified by three sequential identical stages of temperature gradient sublimation using a hot-end temperature of 400 °C, and pressed into pellets. The measurements were performed with the DOLLY and GPS instruments of the Swiss Muon Source at the Paul Scherrer Institut, over a broad temperature range (100–600 K)

using transverse fields above 0.1 T in order to have all paramagnetic signals in the high-field region. In this regime, the muon polarization of a muoniated radical consists of the two f_{12} and f_{43} precession frequencies, each with amplitude of $\frac{1}{2}$ relative to the full asymmetry fraction of the state [5]. The pair of frequencies relates to the hyperfine splitting A of the radical by the sum rule

$$A = f_{12} - f_{43}, \quad (1)$$

where A , considering the hyperfine tensor of the radical to possess axial symmetry, depends on the angle θ defined between the symmetry axis and the external field according to [6]

$$A(\theta) = A_{\text{iso}} + \frac{D}{2}(3 \cos^2 \theta - 1), \quad (2)$$

A_{iso} and D being the isotropic (or hyperfine contact) and dipolar parameters of the hyperfine tensor.

In a polycrystalline sample, θ covers the full solid angle, and a distinctive powder-pattern broadening corresponding to all possible values of A emerges for each of the f_{12} and f_{43} lines in the frequency spectrum [6], as shown in Fig. 2 for all three states I–III in ZnPc.

3. Results: hyperfine parameters

Following the analysis performed in Ref. [2], the time dependence of the muon polarization for the data collected with the ZnPc sample was fitted with a function composed by three independent components describing the signals of states I–III, plus a fourth broad line with the muon Larmor precession frequency, and a fifth small diamagnetic fraction. The polarization of each radical state was now computed as a function of time from the A_{iso} and D fit parameters using a high-field analytical

* Corresponding author at: E.S.Te.S.C., Polytechnic Institute of Coimbra, P-3040-854 Coimbra, Portugal. Tel.: +351 239 802430; fax: +351 239 813395.

E-mail address: piroto@ci.uc.pt (J. Piroto Duarte).

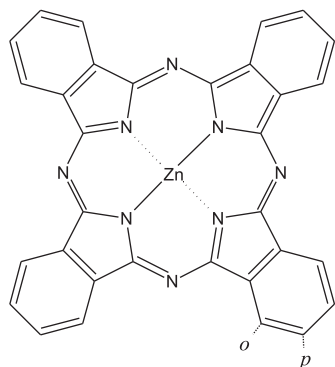


Fig. 1. Molecular structure of the planar phthalocyanine ZnPc. The *p* and *o* indications show, respectively, the *para* and *ortho* addition sites at one of the molecule's outer benzene rings.

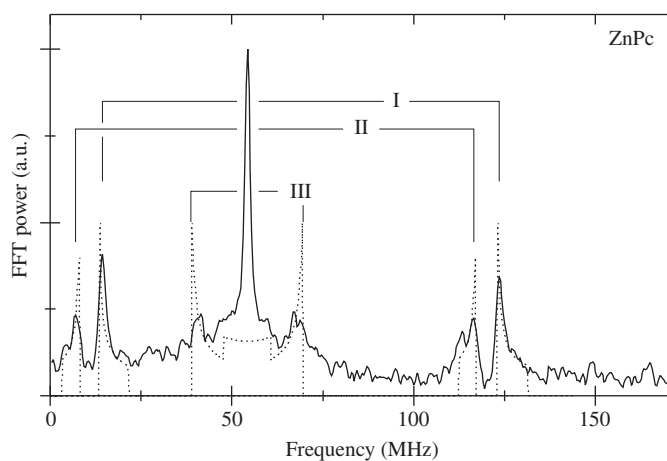


Fig. 2. μ SR frequency spectrum of ZnPc in a field of 0.4T at 500K, with simulated powder distributions (dotted curves) for the line broadening of the paramagnetic states using fitted A_{iso} and D hyperfine parameters.

expression (given in the Appendix) which takes into account the integration over all possible θ angles of Eq. (2). The hyperfine parameters extracted from the time fits are shown as a function of temperature in Fig. 3.

The parameters of state I have the same sign, whereas opposite signs are found for state II. The absolute value of A_{iso} is quite larger than that of D for the two states I and II, and both hyperfine parameters decrease with increasing temperature, the variation of the four parameters being consistent with a temperature-activated behavior of the type [2]

$$A(T) = A_0 + (A_\infty - A_0) e^{-E_a/k_B T}, \quad (3)$$

where E_a is the activation energy of the process responsible for the temperature dependence, and A_∞ and A_0 are the limiting values of $A(T)$ at $T \rightarrow \infty$ and $T = 0$. It must be noted that E_a should not be confused with the temperature coefficient normally used to characterize the temperature dependence of the hyperfine interaction, as it is associated with the relative variation of the hyperfine interaction (regarding the value of $A_\infty - A_0$) rather than with its absolute variation.

For state III, a large dipolar parameter and a small contact interaction is observed, the two bearing opposite signs. Contrary to what happens with states I and II, the hyperfine parameters of state III in ZnPc do not vary significantly with temperature, and are not well fitted by Eq. (3).

Although the noninclusion of additional folding (besides the powder distribution) in the fit components used for states I–III

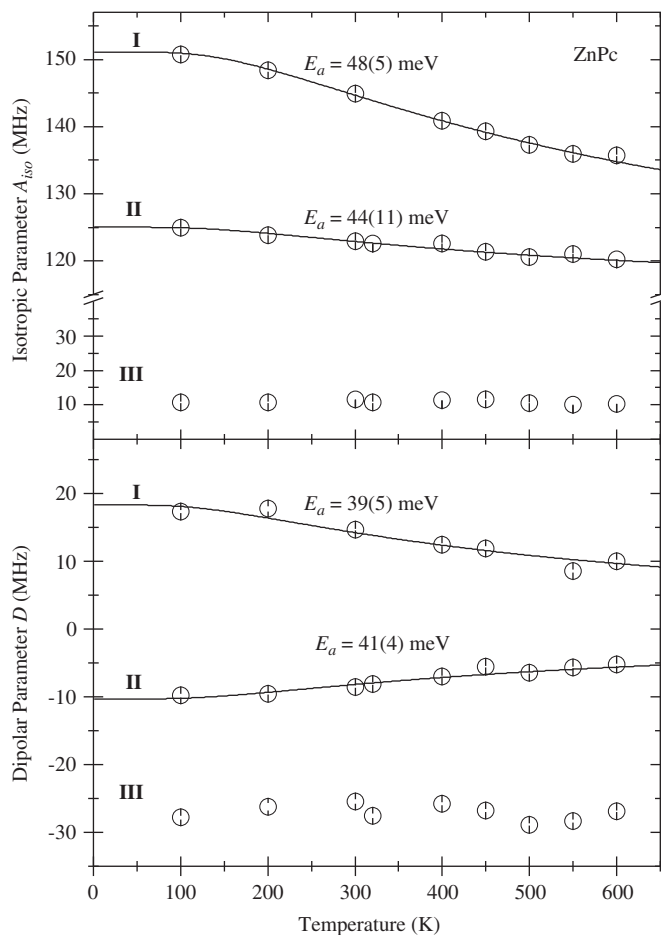


Fig. 3. Temperature dependence of the hyperfine parameters of states I–III in ZnPc considering axially symmetric hyperfine tensors. The solid lines show fits of Eq. (3) to the data of states I and II; for state III, the data follow no relevant temperature dependence (see text).

prevents the reliable estimation of the fractions of each state, it is still possible to perceive from the time fits that state III and the broad fourth component are the dominant components of the signal at all temperatures. They have similar fitted asymmetries, fairly constant throughout the investigated temperature range, and together account for about two-thirds of the observed total amplitude. States I and II exhibit roughly the same amplitude at the highest temperatures, but as temperature decreases below 400K, state II becomes more populated at the expense of state I. Lastly, the asymmetry of the diamagnetic fraction in the signal displays a residual constant value (less than 5% of the total amplitude).

4. Discussion: hyperfine structure and site assignments

4.1. States I and II

According to the electronic structure calculations presented in Ref. [2], states I and II are formed by Mu addition, respectively, at the *para* and *ortho* positions of the outer benzene rings (see Fig. 1). The small dipolar character (low D , when compared with A_{iso}) and the reduced absolute value of the two hyperfine parameters (as compared to the vacuum hyperfine constant of Mu, $A_{\text{hf}}^{\text{vac}} = 4.46$ GHz) for the two states is consistent with a delocalization of the radical electron to the inner double conjugated ring of the phthalocyanine molecule. Also, in those positions, the

Table 1

Energies and expected relative populations at 300 K for the calculated librational modes of the outer carbon rings in ZnPc below 600 cm⁻¹.

Frequency (cm ⁻¹)	Energy (meV)	Relative population (300K)
361.6	44.8	1.00
362.1	44.9	1.00
364.9	45.2	0.98
372.1	46.1	0.95
420.8	52.2	0.75
445.2	55.2	0.67
533.2	66.1	0.44
541.5	67.1	0.42
566.3	70.2	0.37
582.9	72.3	0.35

coupling of the hyperfine interaction of the muoniated radicals with local vibrational modes of the outer rings is the process more likely responsible for the observed temperature variation of the hyperfine parameters.

Since this mechanism implies that the measured activation energies must equal the energies of the modes coupling to the hyperfine interaction, a normal mode analysis of the ZnPc molecule was performed. The computation was done with GAUSSIAN 98 [7] applying the same functionals, pseudo-potentials and wavefunction basis used in Ref. [2], namely the B3LYP electron exchange-correlation functional, the combination of pseudo-potentials from Pascios and Christiansen [8] and the valence basis set from Stevens et al. [9] for the description of the electron core of the C and N atoms, the compact effective potential CEP-31G with double-zeta splitting on the valence for the zinc atom, and the 3-21G basis for the valence electrons. The molecular geometry used was also the optimized geometry calculated in Ref. [2].

The results, presented in Table 1, show that the four lowest energy vibrational modes of the outer rings fall in the region around 45 meV, a value that matches the activation energies observed for the hyperfine parameters of states I and II. All the modes shown are of librational character, implying off-plane relative motion between adjacent carbons in the rings capable of perturbing the σ - π hyper-conjugating effect responsible for the delocalization of the muoniated radical's electron (see e.g. Ref. [5] for a description of this mechanism) in the two states, and hence the value of their hyperfine interactions. Since they are the lowest energy vibrational modes, they are also the most populated ones, and are quite probably the main contributors to the observed temperature variation of the hyperfine parameters of states I and II.

4.2. State III

State III has a peculiar hyperfine structure, exhibiting a dipolar parameter larger than the isotropic parameter, but both with an absolute value which is quite small even for an organic muoniated radical state. This means that the muon is located at a place of naturally low spin density, away from the radical electron, whose wavefunction is highly asymmetrical relative to the muon's position. The similarities of this structure with the electronic structure of the bond-centred muonium (Mu_{BC}) state found in several elemental and compound semiconductors [10] suggest that the muon is in an interstitial site, in-between large electronic wavefunctions. The only muon location consistent with these observations is a position that sits between the centres of two stacked phthalocyanine molecules in consecutive layers, where the muon is sided by the electronic clouds of the inner conjugated ring of those molecules.

5. Conclusions

This work produced detailed information about the hyperfine structure of the paramagnetic muon states formed in ZnPc. It showed that states I and II possess small dipolar parameters with opposite signs, but similar magnitude, and exhibit a temperature variation consistent with the coupling of the hyperfine interaction to vibrational modes of the outer benzene rings of the molecule. For state III, a large dipolar parameter contrasting with a small isotropic parameter of opposite sign was observed, both bearing a temperature dependence which does not fit any energy expected for the vibrational modes of the rings. This fact, supported by the similarity of hyperfine structure with the Mu_{BC} centre, allowed proposing an interstitial position for that state which lies between two stacked phthalocyanine molecules.

Acknowledgements

The assistance of all LMU staff at PSI is gratefully acknowledged. This work was performed at the Swiss Muon Source, Paul Scherrer Institut, Villigen, Switzerland, and partially supported by the European Commission under the 6th Framework Programme through the Key Action: Strengthening the European Research Area, Research Infrastructures, Contract no. RII3-CT-2004-505925. We also thank the support of the Portuguese Foundation for Science and Technology (FCT) through Grant no. POCTI-SFA-2-30 and the PRODEP III program under action 5.3.

Appendix

As it is shown in Ref. [11], the high transverse-field polarization of an axially symmetric paramagnetic muonium state in a randomly oriented polycrystalline sample is given by

$$P_{\mu}(t) = \cos(-\omega_{\mu}t) \left(\frac{FC(\sqrt{3|D|t})}{\sqrt{3|D|t}} \cos\left(2\pi\left(\frac{A_{\text{iso}}}{2} - \frac{D}{4}\right)t\right) - \text{sgn}(D) \frac{FS(\sqrt{3|D|t})}{\sqrt{3|D|t}} \sin\left(2\pi\left(\frac{A_{\text{iso}}}{2} - \frac{D}{4}\right)t\right) \right),$$

where A_{iso} and D are the isotropic and dipolar parameters of the state's hyperfine tensor, ω_{μ} is the positive muon's Larmor precession frequency, sgn means the sign function, and

$$FS(z) = \int_0^z \sin(\pi t^2/2) dt,$$

$$FC(z) = \int_0^z \cos(\pi t^2/2) dt$$

are the Fresnel sine and cosine functions.

References

- [1] Dictionary of Organic Compounds, vol. 5, fourth ed., Eyre & Spottiswoode Publishers, London, 1965.
- [2] J. Pirotto Duarte, et al., Phys. Rev. B 73 (2006) 075209.
- [3] J. Pirotto Duarte, et al., Physica B 326 (2003) 94.
- [4] J. Pirotto Duarte, et al., Physica B 374–375 (2006) 426.
- [5] S.J. Blundell, Chem. Rev. 104 (2004) 5717.
- [6] J.M. Gil, et al., J. Phys. Condens. Matter 13 (2001) L613.
- [7] Computer code GAUSSIAN 98, revision A.9, Gaussian Inc, Pittsburgh, PA, 1998.
- [8] L.F. Pascios, P.A. Christiansen, J. Chem. Phys. 82 (1985) 2664.
- [9] J. Stevens, et al., J. Chem. Phys. 81 (1984) 6026.
- [10] K.H. Chow, et al., in: R.K. Willardson, E.R. Weber, M. Stavola (Eds.), Identification of Defects in Semiconductors, Semiconductors and Semimetals, vol. 51A, Academic Press, San Diego, 1998, pp. 137–207 (treatise).
- [11] J. Pirotto Duarte, Ph.D. Thesis, 2007 (unpublished).